

**GLOBAL AND LOCAL PARTITIONING OF ENERGY RELEASE
RATES IN FEM SIMULATION OF FRMM TEST USING COHESIVE
ZONE**

**GLOBALNA I LOKALNA PODJELA ENERGIJE LOMA U FEM
SIMULACIJAMA FRMM POKUSA PRIMJENOM KOHEZIVNE
ZONE**

Josip Kačmarčik
Mašinski fakultet, Univerzitet u Zenici
Fakultetska 1, Zenica
Bosna i Hercegovina

Aleksandar Karač
Mašinski fakultet, Univerzitet u Zenici
Fakultetska 1, Zenica
Bosna i Hercegovina

Paper categorization: Original scientific paper

ABSTRACT

Finite element simulations of a fixed-ratio mode-mixity test (single configuration) are performed using cohesive zone model. Different simulation parameters are varied: automatic stabilisation, cohesive element viscosity and mesh size. A global and local approach are presented and used for calculation of energy release rate contribution from mode I and mode II fracture in the simulations. The simulations and fracture energy calculation results are evaluated and compared, leading to recommendation for the parameter selection in the finite-element simulation of similar problems.

Keywords: mixed-mode fracture, numerical simulation, FRMM test

SAŽETAK

U radu su sprovedene simulacije, jedne konfiguracije pokusa delaminacije s konstantnim omjerom energija loma pri kombiniranom tipu loma (engl. fixed-ratio mode-mixity test), koristeći metod konačnih elemenata s modelom kohezivne zone. U simulacijama su mijenjani različiti parametri: automatsko stabiliziranje, viskoznost kohezivnih elemenata i veličina mreže. Prikazani su i primijenjeni globalni i lokalni pristup za proračun učešća tipa I i tipa II loma u ukupnoj energiji loma. Sprovedene simulacije i rezultati proračuna energije loma su evaluirani i uspoređeni, iz čega su proistekle određene preporuke za odabir parametara u simulacijama sličnih problema korištenjem metode konačnih elemenata.

Ključne riječi: kombinirani tip loma, numerička simulacija, FRMM pokus

1. INTRODUCTION

This work is conducted as a part of a wider international activity on mixed mode fractures in beam-like geometries under the coordination of European Structural Integrity Society, Technical Committee 4, ESIS-TC4 [1]. The ultimate goal of the project is to develop

(combining analytical, numerical and experimental investigations) a new testing protocol with recommendations for the accurate determination of the fracture mode-mixity.

In the first phase of project, the fixed-ratio mode-mixity test (FRMM) is considered and fracture energy is partitioned analytically and numerically by simulations without damage development [2]. In the second phase, involvement of damage development in simulations is intended, and here, as a preparation (a warm-up case) for the wider investigation, a single FRMM test configuration (Figure 1) delamination is simulated numerically using cohesive zone in commercial software Abaqus, based on finite-element method (FEM).

Since FEM simulations suffer from ever present uncertainties related to the selection of the simulation parameters, present work attempts to shed some light and provide recommendations for the FEM modelling and analyses of delamination in beam-like geometries, in particular the FRMM test, which will be used as guidelines for further investigations of the problem. Simulation parameters which are investigated are: automatic stabilisation, cohesive elements viscosity, and mesh size. The mesh size is in particularly analysed regarding a number of cohesive elements in a damage zone.

For the numerical mixed-mode partitioning, i.e. calculation of energy release rate contribution from mode I and mode II fracture in delamination, a global and a local approach are used and presented. It has to be noted that the term ‘global’ means ‘integration of energy over cohesive zone’, whereas ‘the local approach’ considers ‘integration of energy going into a single cohesive element’.

2. FRMM TEST CONFIGURATION, FEM MODEL AND FEM SIMULATION SETUP

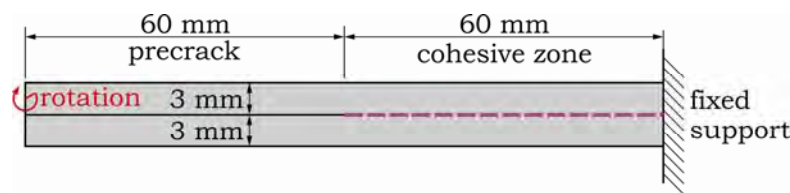


Figure 1. FRMM test configuration.

Figure 1 shows the double cantilever beam (DCB) specimen geometry and FRMM test configuration used in this work. The DCB-FEM model is made from two separate identical beams (parts) with coincident and

connected nodes along a half of the length (dashed line) with zero-thickness cohesive elements (nominal thickness 1). The other half of beams have unconnected coincident nodes, representing the pre-crack. No surface interaction is modelled between beams because two pre-crack surfaces are separated immediately at the test initiation. Abaqus CPE4 (4-node bilinear plane strain quadrilateral) elements are used in two uniform mesh sizes (Figure 2) for modelling beams and COH2D4 (4-node two-dimensional cohesive) elements for modelling cohesive zone. Rotation is applied incrementally at the end of the top beam which is set to be rigid (nodes at the end line are connected into the rigid body) and the other ends of the beams are fixed. Abaqus/Standard one step analysis with geometric nonlinearity accounted is used with the automatic step incrementation. The base model material is linear elastic, isotropic with the modulus of elasticity 50GPa and Poisson’s ratio 0.38.

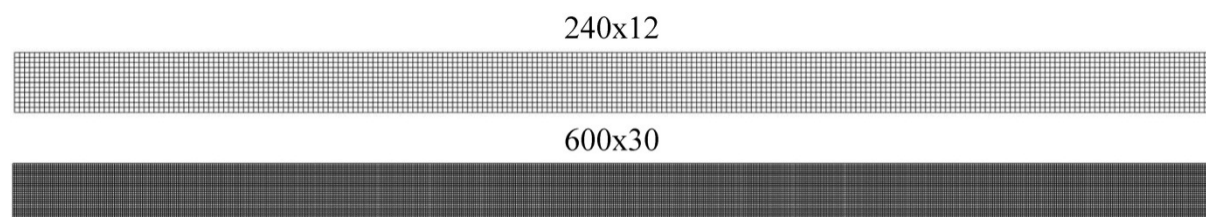


Figure 2. FEM meshes.

2.1. Cohesive traction-separation model

Cohesive zone response is modelled using a traction-separation model, with uncoupled initial linear elastic behaviour that for a two-dimensional problem can be written as [3]:

$$\mathbf{t} = \begin{Bmatrix} t_n \\ t_s \end{Bmatrix} = \begin{bmatrix} K_{nn} & 0 \\ 0 & K_{ss} \end{bmatrix} \begin{Bmatrix} \varepsilon_n \\ \varepsilon_s \end{Bmatrix} = \mathbf{K}\boldsymbol{\varepsilon} \quad \dots(1)$$

where \mathbf{t} is the nominal traction stress vector (normal and shear tractions), \mathbf{K} is the elasticity matrix and $\boldsymbol{\varepsilon}$ is the nominal strain vector. Since nominal strains are defined as separations in two directions (δ_n, δ_s) divided by the nominal thickness that is equal to 1 by default, nominal strains are equal to the separations (see Section 3.1). Uncoupled elasticity matrix is defined with arbitrarily high set value of stiffness $K_{nn} = K_{ss} = 10^{15}$ Pa.

Element damage initiation is defined using the quadratic nominal stress criterion:

$$\left(\frac{t_n}{t_n^o}\right)^2 + \left(\frac{t_s}{t_s^o}\right)^2 = 1. \quad \dots(2)$$

where $t_n^o = t_s^o = 45$ MPa, representing the peak stress values when the deformation is either purely normal or purely in the shear direction (intrelaminar strength).

Damage evolution is described with the scalar damage variable, D , which represents the overall damage in the material. D initially has a value of 0, and after damage initiation monotonically evolves from 0 to 1 in the moment of failure. The stress components of the traction-separation model are affected by the damage according to:

$$t_n = \begin{cases} (1-D)\bar{t}_n, & \bar{t}_n \geq 0 \\ \bar{t}_n, & \text{no damage to compressive stiffness,} \end{cases} \quad \dots(3)$$

$$t_s = (1-D)\bar{t}_s,$$

where \bar{t}_n and \bar{t}_s are the stress components predicted by the elastic traction-separation behaviour for the current strains without damage.

There are quite a few different ways to define damage evolution in Abaqus which differ firstly in a way how the point of complete failure is described: in terms of displacements or energy dissipated. Second difference is how the nature of the evolution of the damage variable, D , between initiation of damage and final failure is specified. The damage evolution laws also include fracture mode-mixity dependence. In this work the linear damage evolution based on energy is used, with critical fracture energy in a value of $G_I^C = G_{II}^C = G^C = 200$ J/m², where dependence of the fracture energy on the mode mixity is given with the power law fracture criterion:

$$\left(\frac{G_I}{G_I^C}\right)^\alpha + \left(\frac{G_{II}}{G_{II}^C}\right)^\alpha = 1, \quad \dots(4)$$

where G_I and G_{II} refer to the work done by the traction in the normal and the shear directions, respectively, and G_I^C and G_{II}^C refer to the critical fracture energies required to cause failure in the normal and the shear directions, respectively.

Using power parameter $\alpha=1$ equation (4) becomes:

$$G_I + G_{II} = G^C, \quad \dots(5)$$

where I and II indicate energy associated with mode I and mode II fracture, respectively.

A more detailed explanation of traction-separation model can be found in [3].

2.2. Convergence improvement techniques

One of the main drawbacks of numerical simulation of delamination in beam-like geometries is that material models exhibiting softening behaviour and stiffness degradation often lead to

severe convergence difficulties. Common techniques to overcome these convergence difficulties are use of viscous regularisation of the cohesive element's constitutive equations and including automatic stabilisation in procedure [3].

Viscous regularisation process involves the use of a viscous stiffness degradation variable, D_v , which is defined by the evolution equation:

$$\dot{D}_v = \frac{1}{\mu}(D - D_v), \quad \dots(6)$$

where μ is the viscosity parameter representing the relaxation time of the viscous system and D is the damage variable evaluated in the backbone model without viscosity. Viscosity regularise the traction-separation laws by permitting stresses to be outside the limits set by the traction-separation law. Using viscous regularisation with a small value of the viscosity parameter (small compared to the characteristic time increment) usually helps improve the rate of convergence of the model in the softening regime, without compromising results. Different values of the viscosity parameter are used and investigated.

Automatic stabilisation is an automatic mechanism for stabilising unstable problems through the automatic addition of volume-proportional damping to the model. The mechanism adds viscous forces of the form:

$$F_v = c \mathbf{M}^* \dot{v}, \quad \dots(7)$$

to the global equilibrium equations, where \mathbf{M}^* is an artificial mass matrix calculated with unit density, c is a damping factor and v is the vector of nodal velocities. The damping factor is defined with a dissipated energy fraction, a small fraction of extrapolated strain energy calculated during the first increment. In the simulations adaptive automatic stabilisation scheme is used, where the damping factor is also controlled by the convergence history and the ratio of the energy dissipated by viscous damping to the total strain energy. The ratio is limited by an accuracy tolerance value imposed on the global level for the whole model. Only default values of 2.0×10^{-4} for the dissipated energy fraction and 0.05 for the accuracy tolerance are used.

A more detailed explanation of convergence improvement techniques can also be found in [3].

3. ENERGY RELEASE RATE CALCULATION

Although energy release rate partitions are included into the cohesive element's damage evolution equations (4), their individual values are not available as Abaqus simulation output variables so they must be calculated by integrating (numerically) outputs for stresses and strains (tractions and separations). Partitioning methods found in literature can be classified as 'local approach' and 'global approach' based on the size of a cohesive zone included in the calculations (one or more cohesive elements).

3.1 Local partitioning: Integration of energy going into a single cohesive element

Mode I and mode II energy release rate components for a point in a cohesive zone can be calculated by integration of traction-separation curves [4]:

$$G_I = \int_0^{\delta_{nm}} \sigma d\delta_n, G_{II} = \int_0^{\delta_{im}} \tau d\delta_t, \quad \dots(8)$$

where δ_{nm}, δ_{im} are maximum (final) opening and shearing displacements of the cohesive elements, δ_n, δ_t are opening and shearing displacements of the cohesive elements and σ, τ are normal and shear stresses (tractions t_n and t_s).

These integrals are numerically calculated using output values for a cohesive element integration point via trapezoidal rule:

$$G_{IP} = \sum_{i=0}^{n-1} \frac{\sigma_i + \sigma_{i+1}}{2} (\delta_{n_{i+1}} - \delta_{n_i}), G_{IIP} = \sum_{i=0}^{n-1} \frac{\tau_i + \tau_{i+1}}{2} (\delta_{i_{i+1}} - \delta_{i_i}), \quad \dots(9)$$

where n is the total number of analysis increments, σ, τ are stress components (Abaqus identifiers s22 and s12) and δ_n, δ_i nominal strain components (Abaqus identifiers ne22 and ne12) for a given increment i ($i+1$). As already mentioned, the values of the strain components are equal to the values of the displacements if the nominal thickness of cohesive elements is set to 1.

Since results obtained with the integrations show quite deviation between two integration points in a cohesive element, relevant values for a cohesive element were finally obtained with averaging values for two integration points in the element:

$$G_I = \frac{G_{IP1} + G_{IP2}}{2}, G_{II} = \frac{G_{IIP1} + G_{IIP2}}{2}, \quad \dots(10)$$

3.2 Global partitioning: Integration of energy over cohesive zone

Once damage region is fully developed, self-similar crack propagation will exist in cohesive zone and the following integrations can then be performed along the cohesive surfaces in order to obtain the global mode I and mode II energy release rates [5],[6]:

$$G_I = \int_0^l \sigma \frac{\partial \delta_n}{\partial x} dx, G_{II} = \int_0^l \tau \frac{\partial \delta_i}{\partial x} dx, \quad \dots(11)$$

where l is the length of integrated cohesive zone, δ_n, δ_i are opening and shearing displacements of the cohesive elements, σ, τ are normal and shear stresses and axis x coincide with a crack propagation direction. Generally, the integration should be done only over the damaged cohesive zone. However, since it is not easily to define the damage zone boundaries, in this work it was more practical to assume longer zone, ie. almost whole cohesive zone, excluding only few cohesive elements at the fixed end (under the influence of the fixed boundary condition). Contributions in the above integrals, from the cohesive elements that have already collapsed or are not damaged, are zero or near zero so they do not have significant influence on the integration results.

Above integrals are numerically calculated using output values for cohesive elements:

$$G_I = \sum_{i=1}^{n-1} \frac{\sigma_i + \sigma_{i+1}}{2} (\delta_{n_i} - \delta_{n_{i+1}}), G_{II} = \sum_{i=1}^{n-1} \frac{\tau_i + \tau_{i+1}}{2} (\delta_{i_i} - \delta_{i_{i+1}}) \quad \dots(12)$$

where n is the number of cohesive element nodes on bottom or top surface of cohesive elements included in integration (with identical values of stress and strain), σ, τ are stress components and δ_n, δ_i are nominal strain components. Values of stresses and strains are averaged to the nodes between adjacent cohesive element integration points, and they are taken in the last increment before the cohesive element in the current crack tip collapses i.e. in the increment when it reaches maximum degradation.

4. ABAQUS SIMULATIONS

4.1. The first set of simulations: viscous regularisation vs. automatic stabilisation

The first set of simulations has been performed to investigate the influence of the viscous regularisation and the automatic stabilisation, as techniques for achieving convergence, on delamination simulations performance (using previously described FRMM test and Abaqus configuration). Although a recommended method for monitoring their influence on an analysis is to compare the energy associated with viscous regulation and automatic stabilisation with overall energy of the model or set of elements and ensure that the ratio does not exceed any reasonable amount [3], a different approach is used in this work. If a steady state crack propagation in FRMM test is achieved, a constant moment acting on an upper

beam (with appropriate motion) should maintain it. Therefore, if the viscosity or stabilisation has no great influence on the stiffness and behaviour in delamination simulation, reaction moment on the rigid body, where boundary rotation is applied, should also be constant in a reasonable range during delamination process. Therefore, a constant trend of the reaction moment after delamination onset is used as a criterion for evaluating accuracy of simulations. Eight FRMM test simulations with different configurations are performed, without and with three different cohesive element viscosity values and with or without including automatic stabilisation (with Abaqus default set-up values). Mesh size for all models is 240x12 (element size 0.5x0.5 mm) and 0.2 rad (11.5°) rotation boundary condition is applied on the top beam end in the 20 second step with automatic incrementation. Beside the reaction moment, following parameters are also evaluated (see Table 1): convergence, number of increments, crack and damage zone propagation length.

Table 1. The first set of simulations configurations and overview of results

Configuration	Stabilisation	Viscosity parameter	Convergence	Increments (automatic)	Crack (mm)	Damage (mm)
A1	NO	0	NO	/	/	/
A2		10^{-1}	YES	23	2	4
A3		10^{-3}	YES	1394	40.5	43
A4		10^{-5}	YES	15728	41	43.5
A5	YES	0	NO	/	/	/
A6		10^{-1}	YES	23	2	4
A7		10^{-3}	YES	151	0.5	2.5
A8		10^{-5}	NO	/	/	/

This set of simulations has shown that for the investigated problem the automatic stabilisation (with default setup) is not a proper convergence improvement technique. The simulations with automatic stabilisation do not converge or the reaction moment after delamination onset is not constant and has physically unrealistic growing trend (see Figures 3 and 4). Conversely, the viscous regulation has shown good results for parameter values of 10^{-3} and 10^{-5} and therefore, value of 10^{-4} is included with those values in the further investigations with different mesh.

Figure 3. Reaction moment for different configurations vs. time/angle

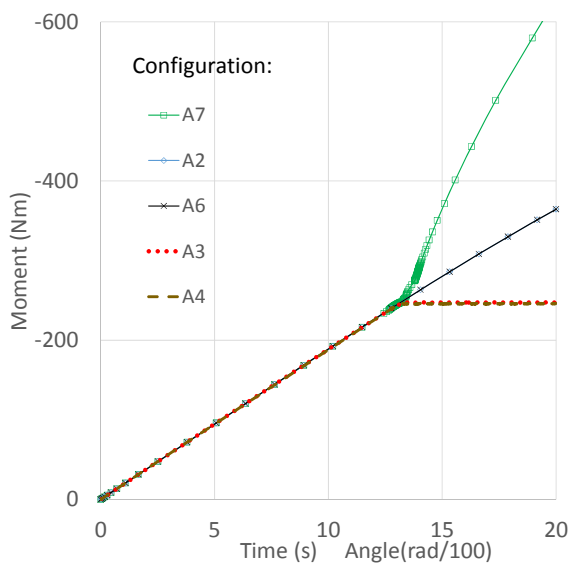
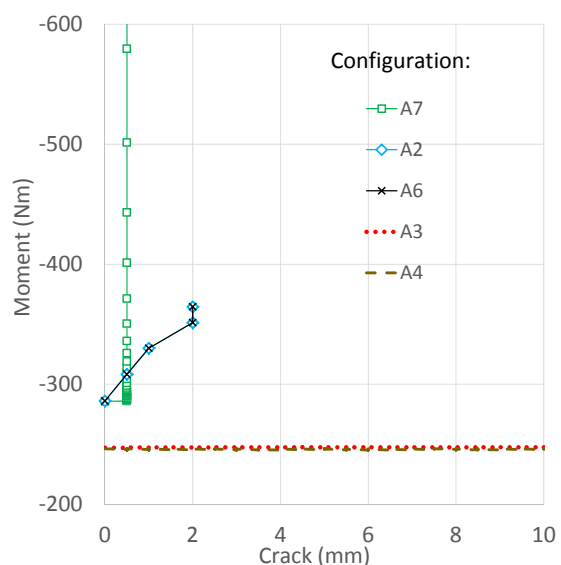


Figure 4. Reaction moment for different configurations in crack propagation



4.2. The second set of simulations: viscosity, mesh size and energy integration method investigation

In this set of simulations viscous regulation is further investigated, including mesh size and integration method selection. Six simulations (see Table 2) with different configurations are carried out and analysed, with three different cohesive element viscosity values (10^{-3} , 10^{-4} and 10^{-5}) and two different mesh sizes: 240x12 (element size 0.5x0.5 mm) and 600x30 (element size 0.2x0.2 mm). The Abaqus output values are imported into a *Microsoft Excel* document where calculation is performed. As can be observed, crack and damage zone propagation as well as size of an initial damage zone for different configurations have close results, what is expected for the simulations with the identical test configurations. All the configurations also have equal (or approximately equal) sizes of the damage zone throughout the delamination process (as expected due to the steady state crack propagation) and also similar values when comparing between them. Based on a size of the initial damage zone and mesh, a number of the elements in a damage zone for each configuration is calculated and considered in further analyses. The reaction moment in all simulations have constant trend during crack propagation (see Figures 5 and 6).

Table 2. The second set of simulations configurations and overview of results

Configuration	Mesh	Viscosity parameter	Convergence	Increments (automatic)	Initial damage zone	Crack (mm)	Damage (mm)	Number of elements in damage zone
B1	240	10^{-3}	YES	1394	2.5	40.5	43	5
B2	x	10^{-4}	YES	6414	2.5	41	43.5	5
B3	12	10^{-5}	YES	15728	2.5	41	43.5	5
B4	600	10^{-3}	YES	993	2	41.2	43.2	10
B5	x	10^{-4}	YES	6837	2.2	42.6	44.6	11
B6	30	10^{-5}	YES	36087	2.2	42.8	44.8	11

Figure 5. Reaction moment for different configurations vs. time/angle

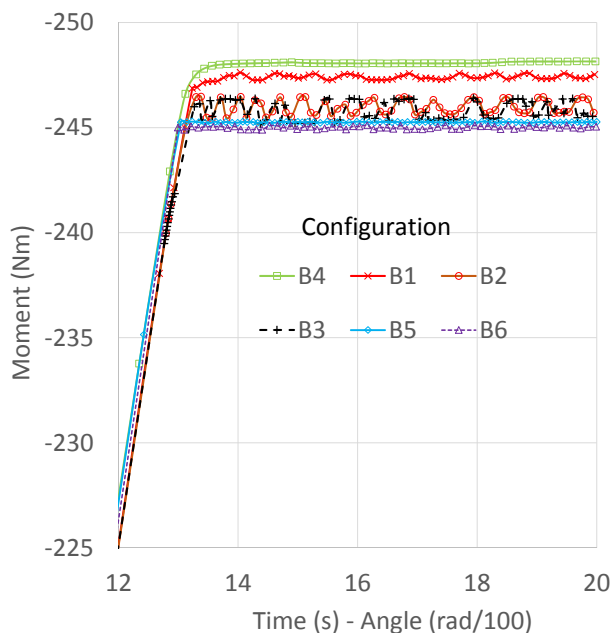
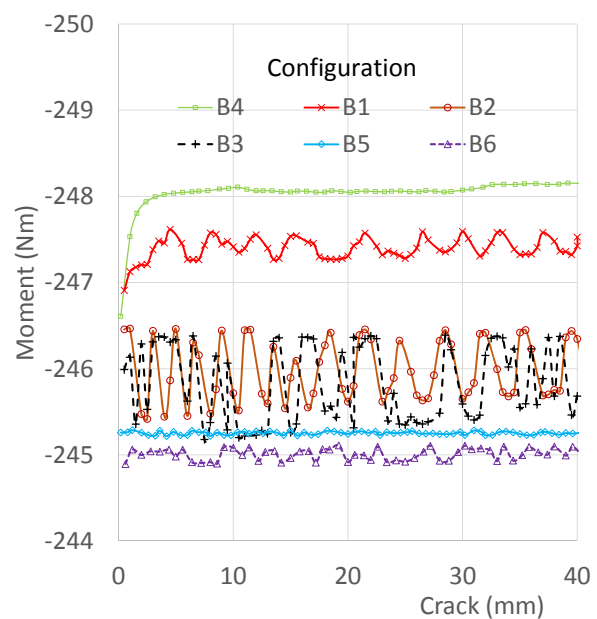


Figure 6. Reaction moment for different configurations in crack propagation



Energy release rates partitions are calculated with previously given equations: (9), (10) and (12), with the two integration methods, in all simulations. Total energy (sum of partitions) calculated by the local and global approach in relation to the crack propagation size is given in Figures 7 and 8, respectively.

The configurations B5 and B6 (with finer mesh and smaller viscosity value 10^{-4} and 10^{-5}) show the smallest error in deviation from the prescribed fracture energy value of 200 J/m^2 . All the charts show converging zone in the crack onset (2 to 5 mm), which is most probably effect of the singularity at the initial crack tip. It can be observed that a converging zone and a change of energy value (as well as error in deviation from the prescribed value) are greater if the viscosity value is higher and the mesh is coarser. Afterwards, a constant trend is observed, with more variations in the results calculated by integration over the cohesive zone for coarser meshes (B1, B2 and B3). The results for these configurations also have greater disagreement in terms of the integration method applied. It can be seen that the global approach is less accurate, what is expected, because a quality of discretisation in a numerical integration for the global approach is directly dependent on a mesh size. A discretisation quality for the local approach is dependent on time increment and common large number of increments provides more accurate calculations. Further mesh refinement is expected to decrease deviations in results from the two calculation methods, but because this would significantly increase CPU processing time, further investigations with the finer mesh were not performed.

Figure 7. Total energy according to the local approach

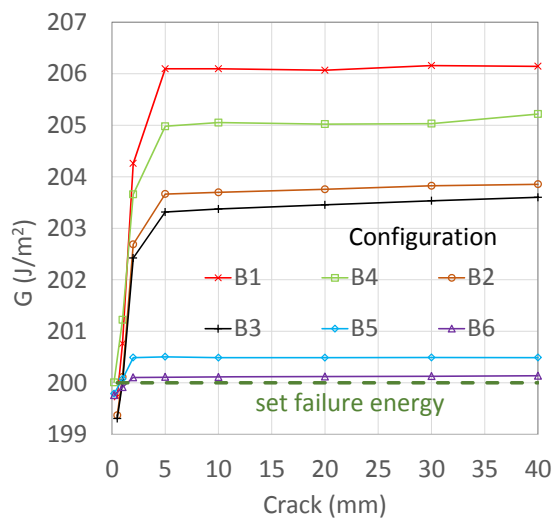
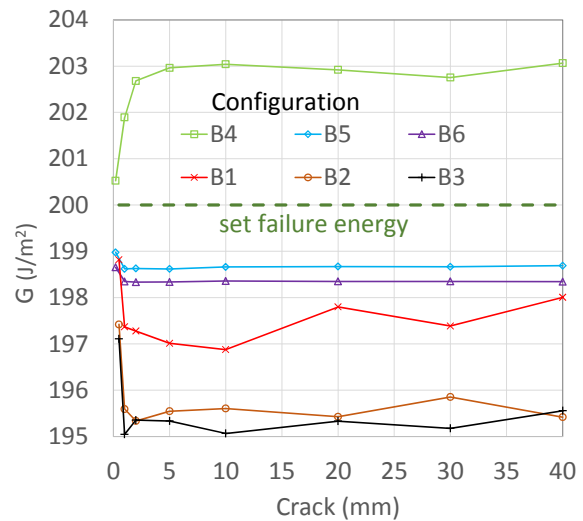


Figure 8. Total energy release rate according to the global approach



Figures 9 and 10 show mode-mixity ratio G_I/G calculated by the local and global approach, respectively, plotted against crack propagation size.

Figure 9. Mode-mixity ratio G_I/G for different configurations calculated by the local approach

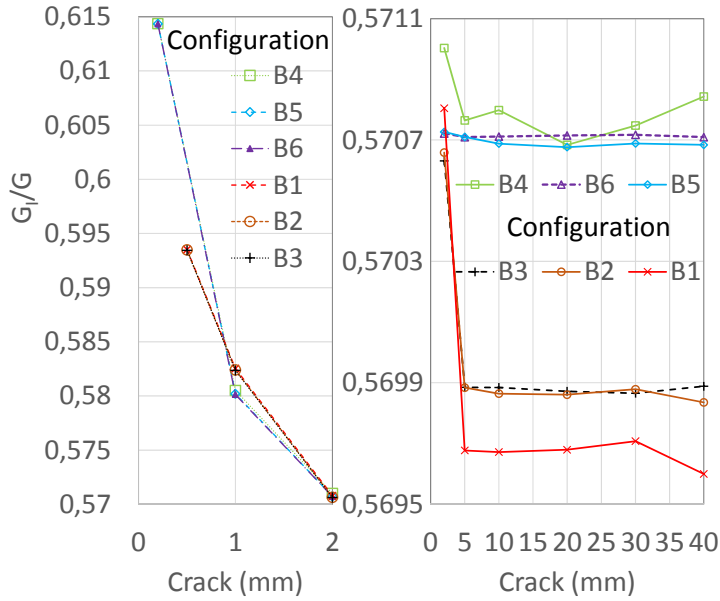
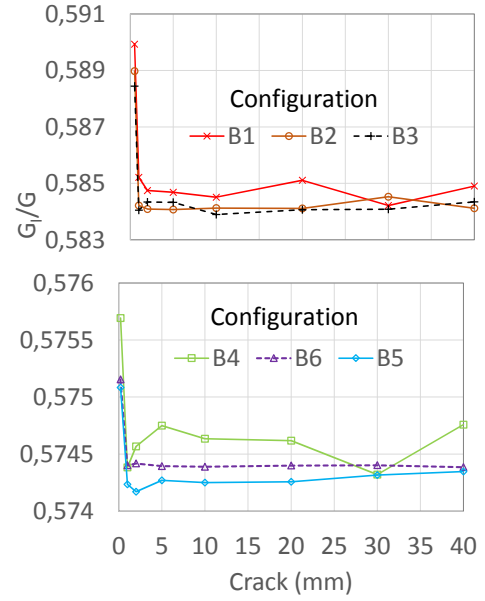


Figure 10. Mode-mixity ratio G_I/G for different configurations calculated by the global approach



The review of the theories and solutions for calculating mode-mixity in beam-like geometries[6]-[11] done in [2] shows that all of them predict almost equal values of G_I/G ratio for the FRMM test configuration used in this work; approximately equal to 0.571. Again, the configurations B5 and B6 provide the most reliable results: the best agreement with analytical solutions and the smallest variations in the crack propagation (proper steady-state behaviour). Similarly to the previous findings from energy calculation, there are larger disagreements between results obtained with different integration methods for the coarse meshes (B1, B2 and B3). Also, converging zone can be observed in the beginning of crack propagation, being larger in the configurations with finer mesh. This shows a change of fracture mode-mixity from a crack tip element (singularity) to the rest of cohesive zone elements that go through similar fracture process. A better insight into the change of mode-mixity with the crack propagation is possible with the local partition approach (in the global approach rest of the zone averages the converging zone), and it shows increasing trend of mode-mixity G_I/G ratio in the crack tip element with mesh refinement.

In summary, the configurations B5 and B6 with mesh size 0.2×0.2 mm and with viscosity values of 10^{-4} and 10^{-5} show the best performance. The recommended mesh size provides 11 elements in the damage zone, what is similar to findings given in [12]. Comparing the two viscosity values, value of 10^{-5} provides slightly better performance, but requires significantly more CPU time (more than 5 times as many increments, table 2), so the value of 10^{-4} is recommended for similar problems.

5. SUMMARY AND CONCLUSIONS

Two simulation sets of a single geometrically symmetrical FRMM test with a pure rotation applied to the top beam have been performed using cohesive zone model in Abaqus. Configurations of the test, FEM model and cohesive zone model used are presented.

The first set of simulations has been used to investigate influence of convergence improvement techniques (viscosity and automatic stabilisation) on simulation accuracy. Cohesive element viscosity is recommended as a better technique for the investigated case. Monitoring of the reaction moment in the nodes where rotation is applied is proposed as an evaluation method.

In the second set of simulations, viscosity values and mesh sizes are varied and their influence on fracture mode-mix analyses is investigated. A global (integration of energy over cohesive zone) and a local (integration of energy going into cohesive element) approach are presented and used for calculation of energy release rate contribution from mode I and mode II fracture. Both approaches give similar results, but the local one provides better insight into change in mode-mixity with crack propagation and shows less mesh dependence. Results lead to the conclusion that the viscosity value of 10^{-4} and a mesh size providing at least 10 cohesive elements in the damage zone can be recommended for similar problems.

The findings presented here will be used in further numerical investigations of FRMM test mode-mixity which will include asymmetric DCB geometries and different cohesive zone properties.

6. REFERENCE

- [1] ESIS TC4 activities, from <http://www.structuralintegrity.eu/tc4-polymers.html>, retrieved March 3, 2014
- [2] B.R.K. Blackman, M. Conroy, A. Ivankovic, A. Karac, A. J. Kinloch, J. G. Williams: Mode-Mixity in Beam-Like Geometries: Linear Elastic Cases and Local Partitioning, ECCM15, 15TH European Conference on Composite Materials, Venice, Italy, 24-28 June 2012
- [3] Abaqus 6.10. Documentation, DassaultSystèmes, 2010
- [4] Q. D. Yang, M. D. Thouless: Mixed-Mode Fracture Analyses of Plastically-Deforming Adhesive Joints, *Int.J.Fract.*110, 175-187, 2001
- [5] M. Conroy, A. Ivankovic, A. Karac, N. Murphy, J.G Williams: Numerical Analysis of mode mixity in Beam Like Geometries using cohesive zones, 12th International Conference on the Science and Technology of Adhesion and Adhesives, York, UK, 4-6 September 2013
- [6] M. Conroy, A. Ivankovic, A. Karac, J.G. Williams: Mode-Mixity In Beam-Like Geometries: Global Partitioning with Cohesive Zones, 36th Annual Meeting of The Adhesion Society, Hilton Daytona Beach, Daltona, FL, USA, 2013
- [7] J. G. Williams: On the Calculation of Energy Release Rates for Cracked Laminates, *International Journal of Fracture Mechanics*, 36, pp. 101-119, 1988
- [8] J.W. Hutchinson, Z. Suo: Mixed Mode Cracking in Layered Materials, *Advances in Applied Mechanics*, 29, pp. 63-191, 1992
- [9] S. Wang, L. Guan: On Fracture Mode Partition Theories, *Computational Material Science*, 52, pp. 240-245 (2012).
- [10] S. Wang, C.M. Harvey: Mixed Mode Partition Theories for One Dimensional Fracture, *Engineering Fracture Mechanics*, 79, pp. 329-352 (2012).
- [11] C.M. Harvey, S. Wang: Experimental Assessment of Mixed-Mode Partition Theories, *Composite Structures*, 96, pp. 758-767 (2012).
- [12] A. Turona, C. G. Davila, P. P. Camanho, J. Costa: An Engineering Solution for Mesh Size Effects in the Simulation of Delamination using Cohesive Zone Models, *Engineering Fracture Mechanics* 74, 1665–1682, 1997